9. Shankar, A., Schroeder, R.J., Wethington, S. M., Graham, C.H., and Powers, D.R. (2020). Hummingbird torpor in context: duration, more than temperature, is the key to nighttime energy savings. J. Avian Biol. *51*, e02305.

10. Laurila, M., and Hohtola, E. (2005). The effect of ambient temperature and simulated predation risk on fasting-induced nocturnal hypothermia of pigeons in outdoor conditions. J. Therm. Biol. *30*, 392–399.

11. Nowack, J., Stawski, C., and Geiser, F. (2017). More functions of torpor and their roles in a changing world. J. Comp. Physiol. B *187*, 889–897.

12. Barratt, A., Welbergen, J., Moore, B., and Turbill, C. (2025). Torpor use in response to predation risk in a small, free-living bird. Behav. Ecol. *36*, araf069.

13. Bondarenco, A., Körtner, G., and Geiser, F. (2014). Hot bats: extreme thermal tolerance in a desert heat wave. Naturwissenschaften *101*, 679–685.

14. Barnes, B.M. (1989). Freeze avoidance in a mammal: body temperatures below 0°C in an Arctic hibernator. Science *244*, 1593–1595.

15. Geiser, F. (2021). Ecological Physiology of Daily Torpor and Hibernation (Switzerland: Springer Nature).

16. Rietbergen, T.B., van den Hoek Ostende, L.W., Aase, A., Jones, M.F., Medeiros, E.D., and Simmons, N.B. (2023). The oldest known bat skeletons and their implications for Eocene chiropteran diversification. PLoS One *18*, e0283505.

17. Geiser, F., Currie, S.E., O'Shea, K.A., and Hiebert, S.M. (2014). Torpor and hypothermia: reversed hysteresis of metabolic rate and body temperature. Am. J. Physiol. *307*, R1324–R1329.

18. Serventy, V. (1970). Torpidity in the white-backed swallow. Emu *70*, 27–28.

19. Congreve, P. (1972). Torpidity in the white-backed swallow. Emu *72*, 32–33.

20. Lovegrove, B.G., Lobban, K.D., and Levesque, D.L. (2014). Mammal survival at the Cretaceous-Paleogene boundary: metabolic homeostasis in prolonged tropical hibernation in tenrecs. Proc. R. Soc. B *281*, 20141303.

Topographic mapping: The making and breaking of adhesive nets

Bérénice Cariou and Iris Salecker*
Institut de Biologie de l'École Normale Supérieure, Université PSL, 46 Rue d'Ulm, 75005 Paris, France
*Correspondence: iris.salecker@bio.ens.psl.eu
https://doi.org/10.1016/j.cub.2026.01.053

Retinotopic maps rely on the spatial preservation of neural adjacencies in the eye and the brain. A new study reveals how such visual maps are established without target-derived cues through a temporal gradient of axon ingrowth and selective axon–axon adhesion.

How we perceive the environment is inseparable from the development of our sense organs and their underlying neural circuits. For instance, to enable spatial encoding of visual information, neighborhood relationships of photoreceptors in the eye are physically preserved by their axons or projections of downstream neurons in the brain[1]. But how do these continuous topographic neural maps arise during development? The first mechanism coming to our minds is very likely the well-established involvement of molecular labels as proposed by the chemoaffinity hypothesis of Roger Sperry[2]. In vertebrates, complementary molecular gradients enable retinal ganglion cell axons to preserve their spatial organization as they find their relative positions in visual processing centers in the brain[1]. In particular, the complex action of Eph receptor kinases and Ephrin ligands has become a classic example in orchestrating retinotectal/retinocollicular map formation through axon–target and axon–axon interactions[3]. Pre-target axon sorting, activity-dependent plasticity and competition equally contribute to visual map formation[4,5]. *Drosophila melanogaster* has emerged as a powerful genetic model for elucidating fundamental principles underlying visual circuit assembly[6]. Cell surface molecule gradients instruct synapse number gradients of higher visual neurons[7]. However, a role for molecular gradients in implementing an anatomical retinotopic map, as has been observed in vertebrates, has remained elusive. In a new study, published in this issue of *Current Biology*, Kehribar *et al.*[8] uncovered an effective alternative strategy that enables photoreceptor growth cones to form a precise retinotopic map by combining temporal differentiation information and local axon–axon adhesive forces.

The fly compound eye consists of ∼750 ommatidia, each containing 8 photoreceptors (R-cells, R1–R8). R7 and R8 axons directly establish a retinotopic map in the second optic ganglion, the medulla during larval and early pupal development. By contrast, R1–R6 axons terminating in the first optic ganglion, the lamina, do so only transiently. R1–R6 axons initially form a regular scaffold of retinotopically organized bundles in a thin layer, called the lamina plexus. Around 25 hours after puparium formation, their growth cones each leave their original fascicles, extending to adjacent columns in a fascinating re-sorting process[9,10]. The outcome is an almost faultless visuotopic organization of adult axonal projections based on the neural superposition principle[11,12]. Ultimately, axon re-sorting ensures that all R-cells that 'see' the same point in space correctly form synapses with identical target neurons in the lamina. It relies on developmental patterning rules that control the synchronous outgrowth, elongation and stopping of thousands of growth cones within a sheet[12–14]. Its successful implementation requires (i) that R-cell axon projections reflect the differentiation pattern in the eye and (ii) that their prior retinotopic organization as starting point is perfect. Indeed, in the eye

imaginal disc, R-cells differentiate and are recruited into rows of ommatidial clusters sequentially[15], followed by the extension of axons through the optic stalk into the optic lobe. Moreover, their targets, lamina neurons, depend on anterograde signals from R-cells to gradually assemble into the correct number of columns and subtypes[16]. Yet, in the absence of these targets, R1–R6 axons are still able to form a remarkably well assembled sheet of self-organizing growth cones that respect the neural superposition wiring pattern[17]. How can R1–R6 growth cones achieve this task in such a dynamically evolving environment?

In the eye imaginal disc, R8 cells first recruit R2/R5 photoreceptors; then R3/R4, followed by R1/R6, and finally R7 join each emerging cluster. These rotate clockwise or anti-clockwise by 90° in the dorsal and ventral halves of the eye field, resulting in a mirror-symmetric arrangement of differentiated R-cells along the equator[15]. Leveraging the fact that ommatidial polarity along the zigzagging equator varies in each animal, Kehribar *et al.*[8] mapped the relative orientations of R-cell clusters in the eye and their axon bundles in the lamina plexus along the dorso-ventral midline and concluded that their patterns perfectly matched, albeit in opposite orientations due to the known 180° torsion of axons[9]. High resolution imaging of the early pupal lamina plexus revealed that R1–R6 axons arrived in the brain in the same order as their cell bodies were recruited into ommatidial clusters in the eye. Importantly, R2/R5 axons arrived first, forming an orthogonal grid in a pattern that was indistinguishable in the dorsal and ventral halves of the lamina plexus prior to the arrival of the other intercalating R-cells within each bundle.

Could this grid form the corner stones of an adhesive net that enables arriving R-cell axons to physically stay in contact with their neighbors? To test this idea, Kehribar *et al.*[8] closely examined the expression of the protocadherin Flamingo (Fmi), a homophilic cell adhesion molecule consisting of cadherin repeats and a seven transmembrane domain. A novel reagent, Fmi-Phluorin-mCherry, made it possible to distinguish expression of active Fmi on membrane surfaces from inactive Fmi in degradative compartments. This genetic trick revealed that the first arriving R8 and R2/R5 axons expressed active Fmi as they navigated through the optic stalk to the lamina plexus. Fmi was then downregulated in axon shafts, but maintained in growth cones within the lamina plexus, ready for its next role during the re-sorting phase[12,13]. Intriguingly, cell-type specific removal of *fmi* in more than five adjacent R8, R2 and R5 axons caused gaps in the lamina plexus. Hence, Fmi plays a dual role in governing inter-bundle adhesion in R2/R5 axons during their trajectory from the eye and in the lamina plexus, to launch retinotopic grid formation. As later arriving R1/R6 axons also express Fmi, they may in turn contribute to the maintenance of the inter-bundle grid.

A closer look using the position of R4 axons as readout revealed that intra-bundle organization had remained intact, leading to the idea that an additional adhesive force is needed to maintain relative axon positions within bundles. The immunoglobulin superfamily member Sidekick (Sdk) stood out as an excellent candidate, as Astigarraga *et al.*[18] had shown that it acts as a homophilic cell

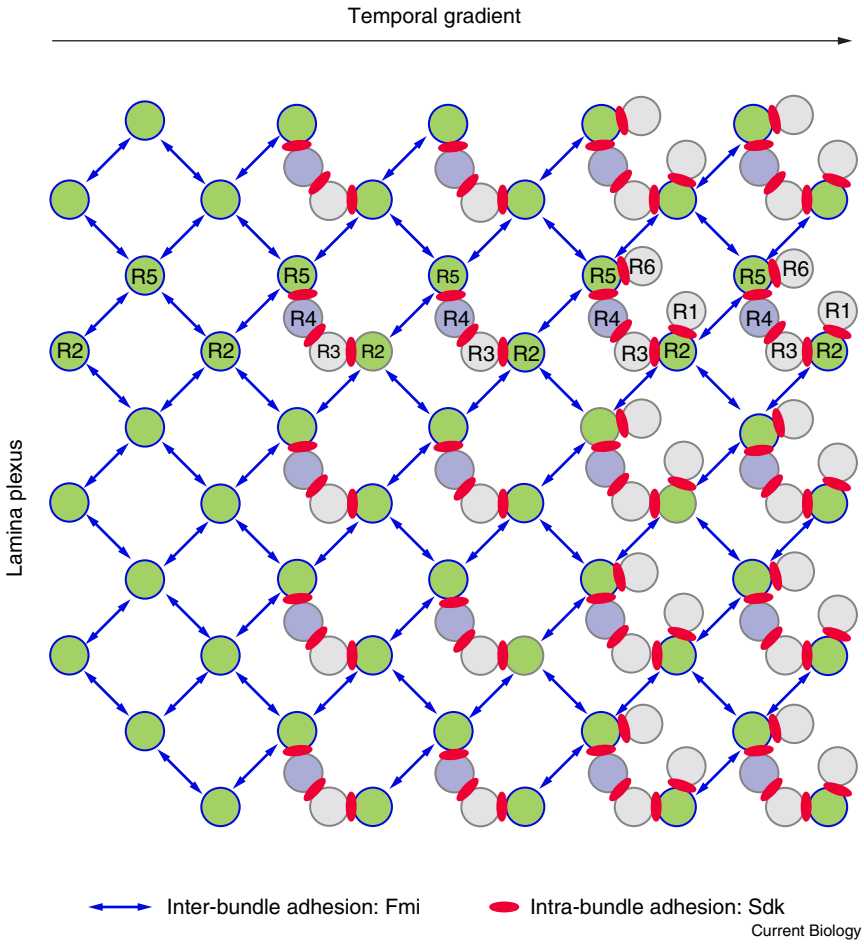

Figure 1. Temporal assembly of a retinotopic map in the visual system of *Drosophila melanogaster* by two adhesive forces.
Rows of R-cell axons arrive in the larval and early pupal lamina plexus gradually, establishing a highly ordered grid of axon bundles. Their arrival order in the lamina plexus reflects that of their recruitment into ommatidial clusters in the developing eye: R2/R5 axons (green) arrive first; young bundles next incorporate R3/R4 axons, while older bundles contain additionally the later arriving R1/R6 axons. Intra-bundle adhesion (blue arrows) is achieved by Flamingo (Fmi) initially between R2/R5 axons (green) to help with setting up the overall grid pattern. Fmi-mediated adhesion between R1/R6 axons is not shown. Sidekick (Sdk) mediates intra-bundle adhesion (red ovals) to preserve the local relative positions of gradually inserting later arriving R-cell axons, such as R4s (violet). Fmi and Sdk establish a gradually forming net, in which spatial proximities are preserved from the eye to the lamina plexus. The schematic illustration shows an area in the dorsal half of the lamina plexus (to simplify the presentation, the changing angles and shapes of R-cell axon bundles in the maturing lamina plexus have not been adjusted).

adhesion molecule, is expressed between R-cell growth cone heel attachment points at the onset of the re-sorting phase, and promotes subsequent growth cone polarization. Focusing on potential earlier developmental roles, Kehribar *et al.*[8] detected Sdk-expression in all R-cell axons as they traveled through the optic stalk. In the absence of *sdk*, R-cell bundles split into smaller bundles, while individual R-cell axons, such as R4s, switched positions within a bundle or between bundles prior to arriving in the lamina plexus, suggesting a distinct role in preserving intra-bundle organization.

How do these forces work in concert? During the third instar larval and early pupal stage, single *fmi* mutant R-cell growth cones did not show any defects. However, large clones resulted in gaps in the larval lamina plexus that were not filled in during pupal development. By contrast, *sdk* loss caused holes in the larval lamina plexus that were corrected during early pupal development but axons remained mispositioned. Only loss of both *fmi* and *sdk* irreparably abolished the structural integrity of the lamina plexus.

In silico simulations provided further support for the distinct contributions of the three tested parameters to robust retinotopic map formation: the gradual row-by-row arrival of R-cell axons, Fmi-mediated R2/R5 inter-bundle forces and Sdk-mediated intra-bundle forces. In addition, the computational model revealed the importance of extensive and flexible interaction surfaces among axons. Thus, the temporal gradient of R-cell development and axon ingrowth could act as a global organizer of topography[1], whereas the two adhesive forces mediated by Fmi and Sdk locally ensure the robust setting up of an orderly scaffold able to integrate new R-cell axons (Figure 1).

In vitro cell assays and structural studies provided evidence that Sdk acts as a homophilic cell adhesion molecule[18,19]. However, while Fmi also is a homophilic determinant, its action seems more complex. It is involved in planar cell polarity of R3/R4 in the eye[20], the setting-up of orderly topographic maps by R2/R5 axons through adhesion and, finally, the re-sorting of R1–R6 growth cones, relying on balancing relative differences in Fmi-mediated activity between neighbors[12,13]. While it is remarkable that genetic analyses can untangle these sequential roles of Fmi, uncovering the underlying molecular basis of this versatility awaits future explorations.

Altogether, these findings extend our conceptual understanding of how visual maps are built beyond guidance to relative positions by chemical gradients: they can rely on the temporal implementation of mechanical forces governed by axon–axon adhesive interactions. Another image would be the gradual tying of a robust net whose knots are held together by two adhesive forces between and within knots. If too many points are weakened, the net may become erroneously assembled, lose its stability and no longer be repairable.

DECLARATION OF INTERESTS

The authors declare no competing interests.

REFERENCES

1. Clandinin, T.R., and Feldheim, D.A. (2009). Making a visual map: mechanisms and molecules. Curr. Opin. Neurobiol. *19*, 174–180. https://doi.org/10.1016/j.conb.2009.04.011.

2. Sperry, R.W. (1963). Chemoaffinity in the orderly growth of nerve fiber patterns and connections. Proc. Natl. Acad. Sci. USA *50*, 703–710. https://doi.org/10.1073/pnas.50.4.703.

3. Weth, F., Fiederling, F., Gebhardt, C., and Bastmeyer, M. (2014). Chemoaffinity in topographic mapping revisited — is it more about fiber-fiber than fiber-target interactions? Semin. Cell Dev. Biol. *35*, 126–135. https://doi.org/10.1016/j.semcdb.2014.07.010.

4. Cioni, J.M., Wong, H.H., Bressan, D., Kodama, L., Harris, W.A., and Holt, C.E. (2018). Axon-axon interactions regulate topographic optic tract sorting via CYFIP2-dependent WAVE complex function. Neuron *97*, 1078–1093.e6. https://doi.org/10.1016/j.neuron.2018.01.027.

5. Li, V.J., Chorghay, Z., and Ruthazer, E.S. (2023). A guide for the multiplexed: The development of visual feature maps in the brain. Neuroscience *508*, 62–75. https://doi.org/10.1016/j.neuroscience.2022.07.026.

6. Malin, J., and Desplan, C. (2021). Neural specification, targeting, and circuit formation during visual system assembly. Proc. Natl. Acad. Sci. USA *118*, e2101823118. https://doi.org/10.1073/pnas.2101823118.

7. Dombrovski, M., Zang, Y., Frighetto, G., Vaccari, A., Jang, H., Mirshahidi, P.S., Xie, F., Sanfilippo, P., Hina, B.W., Rehan, A., *et al.* (2025). Molecular gradients shape synaptic specificity of a visuomotor transformation. Nature *644*, 453–462. https://doi.org/10.1038/s41586-025-09037-4.

8. Kehribar, M., Wit, C.B., Krasikova, K., Agi, E., Reifenstein, E.T., Wolterhoff, N., Wriedt, L.Q., von Kleist, M., and Hiesinger, P.R. (2026). Selective adhesion preserves eye patterning as axonal retinotopy in the Drosophila brain. Curr. Biol. *36*, 1097–1114.e6.

9. Meinertzhagen, I.A., and Hanson, T.E. (1993). The development of the optic lobe. In The Development of Drosophila melanogaster, M. Bate, and A. Martinez Arias, eds. (Cold Spring Harbor Laboratory Press), pp. 1363–1491.

10. Clandinin, T.R., and Zipursky, S.L. (2000). Afferent growth cone interactions control synaptic specificity in the Drosophila visual system. Neuron *28*, 427–436.

11. Horridge, G.A., and Meinertzhagen, I.A. (1970). The accuracy of the patterns of connexions of the first- and second-order neurons of the visual system of Calliphora. Proc. R. Soc. Lond. B Biol. Sci. *175*, 69–82. https://doi.org/10.1098/rspb.1970.0012.

12. Schwabe, T., Neuert, H., and Clandinin, T.R. (2013). A network of cadherin-mediated interactions polarizes growth cones to determine targeting specificity. Cell *154*, 351–364. https://doi.org/10.1016/j.cell.2013.06.011.

13. Chen, P.L., and Clandinin, T.R. (2008). The cadherin Flamingo mediates level-dependent interactions that guide photoreceptor target choice in Drosophila. Neuron *58*, 26–33. https://doi.org/10.1016/j.neuron.2008.01.007.

14. Langen, M., Agi, E., Altschuler, D.J., Wu, L.F., Altschuler, S.J., and Hiesinger, P.R. (2015). The developmental rules of neural superposition in Drosophila. Cell *162*, 120–133. https://doi.org/10.1016/j.cell.2015.05.055.

15. Wolff, T., and Ready, D.F. (1993). Pattern formation in the Drosophila retina. In The Development of Drosophila melanogaster, M. Bate, and A. Martinez-Arias, eds. (Cold Spring Harbor Laboratory Press), pp. 1277–1325.

16. Apitz, H., and Salecker, I. (2014). A challenge of numbers and diversity: neurogenesis in the Drosophila optic lobe. J. Neurogenet. *28*, 233–249. https://doi.org/10.3109/01677063.2014.922558.

17. Agi, E., Reifenstein, E.T., Wit, C., Schneider, T., Kauer, M., Kehribar, M., Kulkarni, A., von Kleist, M., and Hiesinger, P.R. (2024). Axonal self-sorting without target guidance in Drosophila visual map formation. Science *383*, 1084–1092. https://doi.org/10.1126/science.adk3043.

18. Astigarraga, S., Douthit, J., Tarnogorska, D., Creamer, M.S., Mano, O., Clark, D.A., Meinertzhagen, I.A., and Treisman, J.E. (2018). Drosophila Sidekick is required in developing photoreceptors to enable visual motion detection. Development *145*, dev158246. https://doi.org/10.1242/dev.158246.

19. Goodman, K.M., Yamagata, M., Jin, X., Mannepalli, S., Katsamba, P.S., Ahlsen, G., Sergeeva, A.P., Honig, B., Sanes, J.R., and Shapiro, L. (2016). Molecular basis of sidekick-mediated cell-cell adhesion and specificity. eLife *5*, e19058. https://doi.org/10.7554/eLife.19058.

20. Das, G., Reynolds-Kenneally, J., and Mlodzik, M. (2002). The atypical cadherin Flamingo links Frizzled and Notch signaling in planar polarity establishment in the Drosophila eye. Dev. Cell *2*, 655–666. https://doi.org/10.1016/s1534-5807(02)00147-8.